

An integrated geophysical analysis of crustal structure in the Wichita Uplift region of southern Oklahoma

Amanda (Rondot) Buckey

*Gulf of Mexico Exploration – Paleogene, Marathon Oil Company, 5555 San Felipe Street, Houston, Texas 77056.
anbuckey@marathonoil.com.*

ABSTRACT

The Southern Oklahoma Aulacogen (SOA) is a northwest-trending failed arm of a Cambrian triple junction. Significant structures along the SOA include the Wichita Uplift and the Anadarko Basin in southwest Oklahoma. The rift underwent a complex geologic history of bimodal volcanism, faulting, and subsidence before Pennsylvanian compression inverted and uplifted the structure as part of the formation of the Ancestral Rocky Mountains.

This study employed data from a wide-aperture seismic survey shot in 1985 across the Hardeman Basin, Wichita Uplift, and the Anadarko Basin as a joint effort between the University of Texas at El Paso (UTEP) and the University of Texas at Dallas (UTD). Using modern software and processing techniques, I picked numerous refracted and reflected phases and then performed ray-tracing modeling of these picks to build a P-wave seismic-velocity model of the upper crust underneath the Wichita Uplift. I integrated the seismic data with gravity and magnetic data, well data, industry reflection data, and the results of previous studies to arrive at my final geologic model, which includes well-constrained fault locations.

This model shows that the granite and rhyolite sequence present beneath the uplift is thicker and more continuous than previously modeled. Thick sequences of what may be metasediments are present adjacent to the Proterozoic basin at the southern end of the model. Dense mafic layers extending to a depth of 15 km form the core of the uplift, revealing the impressive scale of crustal modification in the rifting process.

INTRODUCTION

The Southern Oklahoma Aulacogen (SOA) is a classic example of an aulacogen (failed rift), as interpreted by Shatski (1946) and Hoffman et al. (1974) and revisited by Keller and Stephenson (2007). The aulacogen trends to the northwest from the Cambrian rifted margin of Laurentia in northeast Texas, across southwestern Oklahoma, and possibly into Colorado and Utah (Figure 1). Geologic evidence for this feature is obscured in the southeast end by deformation from the Ouachita orogeny (Keller et al., 1983) and in the northwestern end by Laramide deformation (Larson et al., 1985). Major structures associated with it include the Wichita-Amarillo Uplift, Arbuckle Uplift, and Anadarko Basin, the deepest sedimentary basin in North America and a prolific hydrocarbon-producing area (Gilbert, 1983).

My study utilizes the data set from a 1985 wide aperture reflection/refraction seismic survey obtained across the Hollis-Hardeman Basin, the Wichita Uplift, and the Anadarko Basin by the University of Texas at El Paso (UTEP) and the University of Texas at Dallas (UTD). The survey consisted of nine in-line shotpoints and eight off-line shotpoints, with several shots repeated using different

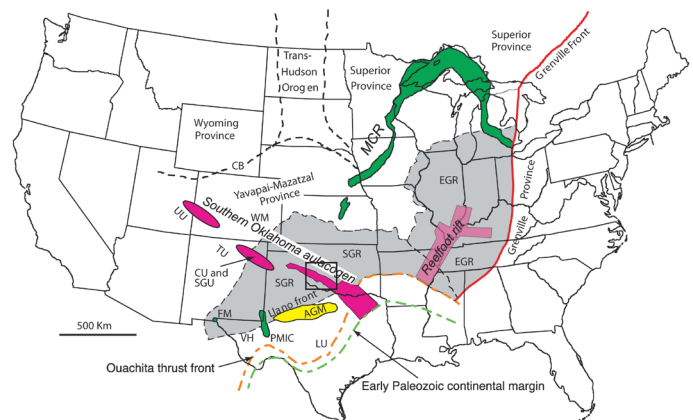


Figure 1. Location of the Southern Oklahoma Aulacogen. The approximate study area is indicated by the black box. Modified from Keller and Stephenson (2007).

recorder deployments. The in-line shots have been analyzed by Zhu and McMechan (1989), Hamilton (1989), Hsueh (1991), and Suleiman (1993) to construct two-dimensional velocity models across the Wichita Uplift and the Anadarko Basin. Chang et al. (1989) also generated a prestack depth-imaged model across the majority of the survey line using twelve of the inline shot gathers.

However, the off-line shots have not been studied in detail until my study due to the absence of necessary software. I was able to produce a new set of seismic record sections and enhance these data with a variety of filters in order to provide improved phase identifications. This approach produced considerably more identifiable phases and picks for modeling than previous studies did.

The goals of this study are: 1) to create a more detailed model of the upper crust of the Wichita Uplift and evaluate its geologic interpretation, 2) to employ first- and later-arrival-time picks to perform ray tracing and inversion on the shot gathers, 3) and to produce an integrated model that will be constrained by previous models, well data, industry reflection images, and gravity and magnetic data.

Geologic Setting

An aulacogen is a linear structural trough that extends at a high angle from a continental margin or an orogenic belt into the continental platform (Hoffman et al., 1974). The SOA displays many of the commonly recognized characteristics of such features, including an early history as a large graben, the occurrence of bimodal rhyolitic and basaltic rocks, and later reactivation and structural inversion (Burke, 1977).

Hoffman et al. (1974) and Burke and Dewey (1973) presented a hypothesis for the origin and development of aulacogens within a plate tectonics context. A mantle plume beneath a continent causes a domal uplift to form, which breaks apart into a three-armed rift system. Two of the rift arms continue to separate to form an ocean basin, while the third arm is abandoned. The "failed" arm will maintain a graben form and be injected with volcanics while the mantle upwelling continues. Once upwelling diminishes and ceases, the domal uplift sinks into a broad downwarp due to thermal contraction of the crust, and the graben collapses inward. The normal faults become high-angle reverse faults, and the crust of the central block is thickened. Rift zones form regions of weakness which are prone to later structural reactivation (Burke and Dewey, 1973). Hoffman et al. (1974) also observed that aulacogens may control sedimentation patterns after the aulacogen itself is no longer active.

The SOA comprises one of the most extensive exposures of igneous rocks within the mid-continent (McConnell and Gilbert, 1990). Ham et al. (1964) described in detail the exposed igneous and metamorphic rocks around the Wichita Mountains. The geology of the SOA can be divided into three stages spanning ~1200 Ma: 1) pre-rift, 2) active rifting from Middle Cambrian until Late Mississippian, and 3) post-rift deformation including Pennsylvanian compression and Pennsylvanian-Permian strike-slip faulting (Gilbert, 1983).

The aulacogen formation likely initiated along a pre-existing structural weakness, possibly a Proterozoic northwest-trending arch across the Midcontinent (Gilbert, 1983) or a Precambrian fault bounding the Proterozoic basin to the south (Brewer et al., 1983) through a Precambrian granitic basement. The Tillman Metasedimentary Group is the oldest unit assigned to the Wichita province. Early studies suggested that it was deposited on top of an eroded granitic basement, marking the beginning of basin formation (Ham et al., 1964). This group may compose all or part of the sedimentary fill in the Proterozoic basin inferred to underlie the Hardeman Basin (Brewer et al., 1981). The Tillman Metasedimentary Group is known only from the subsurface in an area south of the Wichita Mountains (Ham et al., 1964).

Rifting began in the late Proterozoic-Early Cambrian as the Proto-Atlantic Ocean opened (Gilbert and Hogan, 1995). The rise of tholeiitic basaltic magma is assumed to indicate the commencement of rifting, forming the Raggedy Mountain Gabbro Group and the Navajoe Mountain Basalt-Spilitic Group. The Raggedy Mountain Gabbro Group consists of two intrusive formations, the Glen Mountain Layered Complex (GMLC) and the Roosevelt Gabbros. The Navajoe Mountain Basalt-Spilitic Group is the extrusive equivalent of the GMLC, having been deposited as shallow submarine flows on top of Tillman graywackes (Ham et al. 1964).

The Roosevelt Gabbros form a series of smaller, internally differentiated plutons that intrude the GMLC (McConnell and Gilbert, 1990). Subsequent to or concurrent with Roosevelt Gabbro emplacement, uplift and erosion removed 2-4 km of the Raggedy Mountain Gabbro Group and an unknown amount of sedimentary overburden (Powell and Phelps, 1977).

Carlton Rhyolite extruded onto the erosional surface above the gabbros while its intrusive equivalent, the Wichita Mountain Granite, crystallized at shallow depths. The Carlton Rhyolite is composed of a series of rhyolitic flows with interbedded water-laid tuff, agglomerate, and welded

tuffs (Ham et al., 1964). Its distribution trends northwest, paralleling the strike of the inferred bounding faults of the rift zone (Gilbert, 1983). The lavas likely erupted out of linear fissures within a half-graben setting with subsidence to the north, as the rhyolite is over 1400 m thick north of the Wichita Mountains but absent to the south (McConnell and Gilbert, 1990). Within the central Wichita block, the Wichita Mountain Granite formed plutons and sills injected between the Raggedy Mountain Gabbro Group and the Carlton Rhyolite (Ham et al., 1964).

Finally, a series of late diabase plugs and dikes cut all other igneous units. However, the intrusions do not cut across the overlying unconformity into the Upper Cambrian sediments, constraining the end of igneous activity within the aulacogen (Gilbert, 1983). Trace-element signatures indicate the magma source originated within a mid-crustal layered mafic complex (McConnell and Gilbert, 1990).

Two major models have been proposed for the tectonic evolution of the SOA. Hoffman et al.'s (1974) model presents a generalized overview of the SOA development as an example of aulacogen formation. The process begins with rifting to form grabens and half-grabens which are filled with igneous rocks and sediments. Regional sagging centered over the rift zone creates a basin for the widespread deposition of sediments. Finally, reactivation of the rift-related faults as reverse faults deforms and uplifts the sequence. Gilbert (1983) conceived a more detailed series of evolutionary stages for the SOA in specific that incorporates the specific igneous geology of the region (Figure 2).

Following the end of igneous activity and accompanying reduction in heat flow, a period of thermally controlled subsidence and sediment accumulation occurred (Feinstein, 1981) in which 4-5 km of carbonates, then clastics, were deposited. The Anadarko Basin is depicted as forming centered over the rift zone (Gilbert, 1983), although little evidence has been presented that delineates the location of the rift edges at this time. Basin depocenters progressively moved north during the Silurian to Mississippian. Finally, crustal shortening in the early Pennsylvanian uplifted the igneous core of the Wichita Mountains through reactivation and inversion of rift-related normal

faults. The Anadarko Basin continued subsiding after uplift of the igneous block ceased as material eroded from the uplifted block was deposited into the Anadarko Basin, creating over 12 km of structural relief between the uplift and the basin (Gilbert, 1983).

The SOA composes one of the major elements of the Ancestral Rocky Mountains, a series of fault-bounded basement uplifts and flanking basins formed in the Late Mississippian to Permian that stretches from Oklahoma to Utah (Kluth and Coney, 1981). The driving stresses of this intracratonic deformation are under debate.

An understanding of the deformation characteristic of the SOA may provide insights on the formation of the Ancestral Rocky Mountains. Various studies agree that defor-

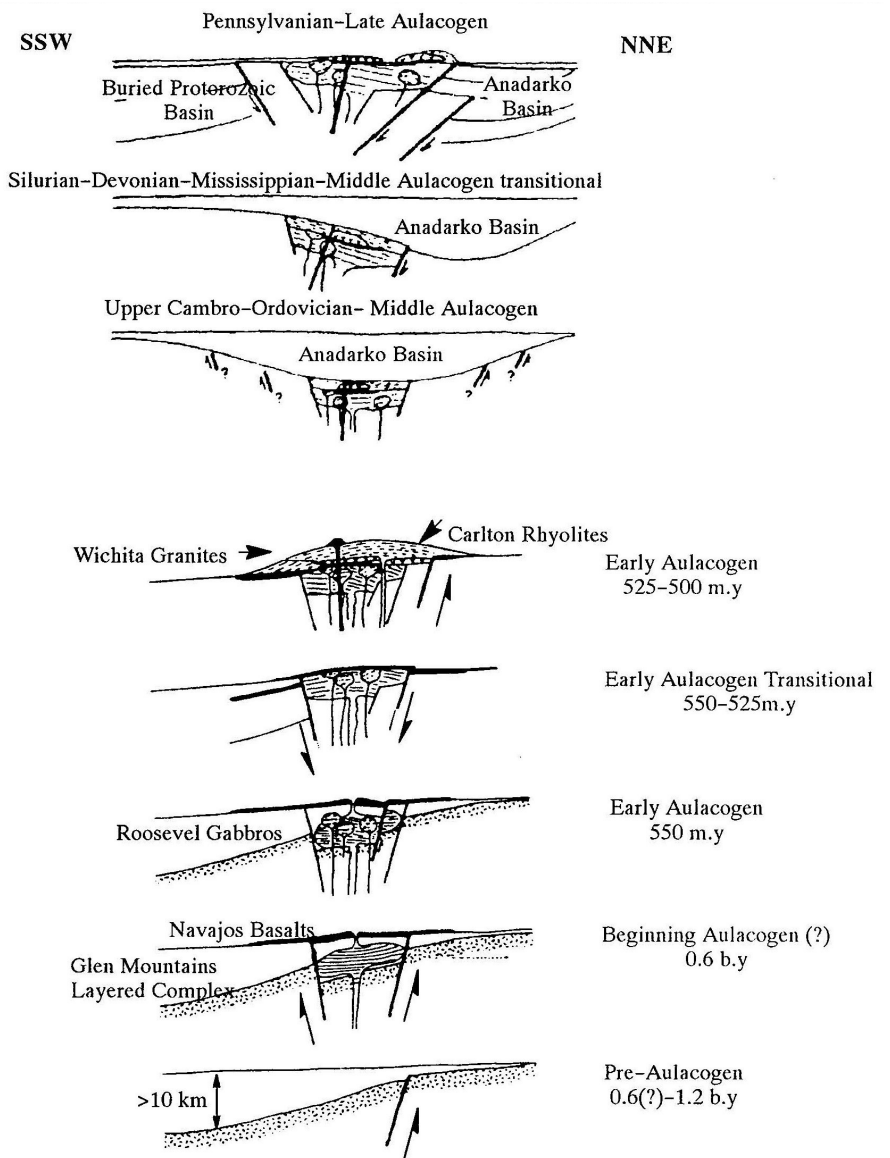


Figure 2. Gilbert's (1983) model of the tectonic evolution of the SOA.

mation likely occurred along pre-existing zones of weakness; however, opinions differ on the scale of these zones. Geologic observations along the frontal fault zone between the Wichita Uplift and the Anadarko Basin show that the faults have both left-lateral strike-slip and reverse senses of motion (Budnik, 1986). Although some workers have proposed that 100-150 km of left-lateral slip occurred along this zone (Budnik, 1986), more recent palinspastic reconstructions in southwest Oklahoma indicate that only 12-26 km of slip occurred, an amount approximately equal to the magnitude of reverse slip (McConnell, 1989). This smaller magnitude lends support to Kluth and Coney's (1981) interpretation that deformation occurred along discrete fault zones bounding separate uplifts, rather than along one major zone as proposed by Larson et al. (1985) and Budnik (1986).

Previous Geophysical Studies

Numerous commercial seismic surveys have been shot through the Anadarko Basin region for hydrocarbon-exploration purposes, although little of this data has been published. Widess and Taylor (1959) utilized a line of 22 shotpoints across northern Comanche County and southern Caddo County to study seismic reflections from layering within the basement north of the Wichita Uplift. Although their record sections extended to only three sec in time, they utilized data from the Pan Am No. 1 Perdasofpy well to show that the continuous, gently dipping reflections that appeared to be sedimentary horizons or multiples from overlying sedimentary horizons are actually layered silicic and gabbroic igneous rocks.

Additionally, several academic seismic surveys have been conducted across the Wichita Uplift and surrounding regions to image the deep crustal structure (Figure 3). A 1964 deep seismic experiment employed two shotpoints, one near the Wichita Uplift and one in northeast Oklahoma, with 37 recording locations to provide a low-resolution image of the crustal structure across the central portion of Oklahoma, as modeled by Tryggvason and Qualls (1967). Mitchell and Landisman (1970) integrated this seismic data set with gravity data, geological observations, and well-log data to determine a crustal thickness of approximately 46 km across the section. They divided the crust into two general regions, an upper crust and a deeper crustal region. They also proposed that major crustal movements have been limited to the upper crust, based on two seismic interfaces above 17 km being broken by major faults, whereas four continuous interfaces below 17 km were identified.

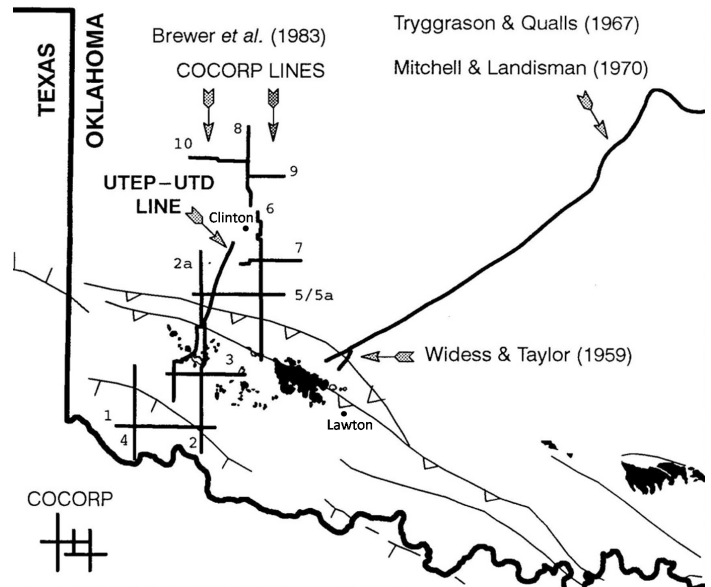


Figure 3. Map showing the locations of non-industry seismic acquisitions in Oklahoma. Modified from Suleiman (1993).

The Consortium for Continental Reflection Profiling (COCORP) recorded several deep seismic-reflection lines across the Hardeman Basin just south of the Oklahoma border in northern Texas (1975), the Hardeman Basin in Oklahoma and the Wichita Uplift (1979), and the Wichita Uplift into the Anadarko Basin (1980). Lynn (1979) studied the time-migrated sections from the Texas Hardeman Basin experiment. Well data places the top of the rhyolite basement at 1.4 sec, with well-defined sedimentary reflectors above this time. A seismically transparent zone occurs between 1.6 and 2.8 sec, and high-amplitude continuous reflectors are seen at 2.8 and 3.8 sec. Lynn (1979) interprets these reflectors as evidence of a silicic complex ~7.5 km thick composed of tuff and volcanic flows that generate layered reflections grading downward into a pluton of seismically transparent granitic rocks. Between 3.8 sec and 11 sec, discontinuous reflectors less than 1 km in length with varying dips interpreted as metasediments, amphibolites, and migmatites occur.

However, similar layering seen just to the north in the Hardeman Basin on the 1979 lines was interpreted as a Proterozoic basin filled with bedded metasediments, likely the Tillman Metasedimentary Group, and felsic volcanics underlying the Paleozoic basin (Brewer et al., 1981; Pratt et al., 1992). The base of the Paleozoic section occurs at 1.3 sec (~3 km), underneath which two strong continuous reflections are seen at 2.9 sec (~7.5 km) and 3.5 sec (~10 km). These reflections are truncated near the southern edge

of the Wichita Uplift, likely due to a Precambrian bounding fault. A strong discontinuous event at 5 sec (~13 km) appears to truncate beds below it and is interpreted as an erosional unconformity. Other continuous events of moderate amplitude appear to onlap and downlap onto lower horizons, suggesting depositional horizons of either a clastic sedimentary or volcanic flow nature (Brewer et al., 1981).

Interpretations of the 1980 COCORP profiles by Brewer et al. (1983) suggest that remnants of the Precambrian layered sequence under the Hardeman Basin may be present under the Wichita Uplift in the form of faulted discontinuous reflectors. However, this thick sequence is not seen under the Anadarko Basin.

The most recent academic data set was obtained from a wide-angle reflection/refraction survey conducted in 1985 by the University of Texas at El Paso and the University of Texas at Dallas across the Oklahoma portion of the Hardeman Basin, the Wichita Uplift, and into the Anadarko Basin. Multiple studies have been conducted using this data set. Chang et al. (1989) created a 2-D velocity model using prestack depth-migrated data. This model shows that the Wichita Uplift is generally seismically transparent, though several reflectors are identifiable. A zone of increased reflectivity, possibly representing a zone of crustal underplating, begins at 28 km depth. The P-wave velocities imply that the uplift is underlain primarily by mafic material; velocities under the uplift are ~25% faster than in the Anadarko Basin. The uplift-basin transition zone shows evidence of thrust faulting extending down to at least 30 km, where the authors interpret a ductile detachment zone separating thrust-faulted upper and middle crust from thickened lower crust. The Anadarko Basin also contains a dense series

of reflectors down to 30 km, with less coherent reflectors visible to a depth of 45 km. A strong reflector at 17 km that shallows to 14 km towards the north is inferred to represent the bottom of the basin.

Zhu and McMechan (1989) developed a 2-D P-wave velocity model to a depth of ~15 km. They found that the average velocity within the uplift is more typical of middle rather than upper crustal material. The core of the uplift is composed of a high-velocity (>6.8 km/sec) material, likely intrusions from the lower crust and upper mantle, whereas a low-velocity region that may be a remnant of normal crust resides at a depth of ~5 km. Kang and McMechan (1990) found similar results, but with more detail.

Hamilton (1989) studied the structure under the Wichita Uplift. Traveltime inversion of first-arrival picks shows that velocities are distributed asymmetrically underneath the uplift with higher velocities found toward the north, likely corresponding to gabbroic bodies. Combining velocity inversion with ray tracing yielded a 2-D model of seven interfaces extending down to a depth of ~13 km (Figure 4). Hsueh (1991) extended Hamilton's model across the frontal fault zone into the Anadarko Basin (Figure 5). His work showed that the Anadarko Basin is strongly asymmetrical; the top of normal upper crust (Precambrian basement) is interpreted to lie at a depth of 8 km beneath the northernmost shotpoint used and dip southward to a depth of 15 km in the deepest portion of the basin.

Suleiman (1993) built upon Hamilton and Hsueh's studies to determine the deep crustal structure underneath the length of the survey line. This study concluded the crustal thickness increases below the Wichita Uplift into the Anadarko Basin, with a maximum thickness of 45 km.

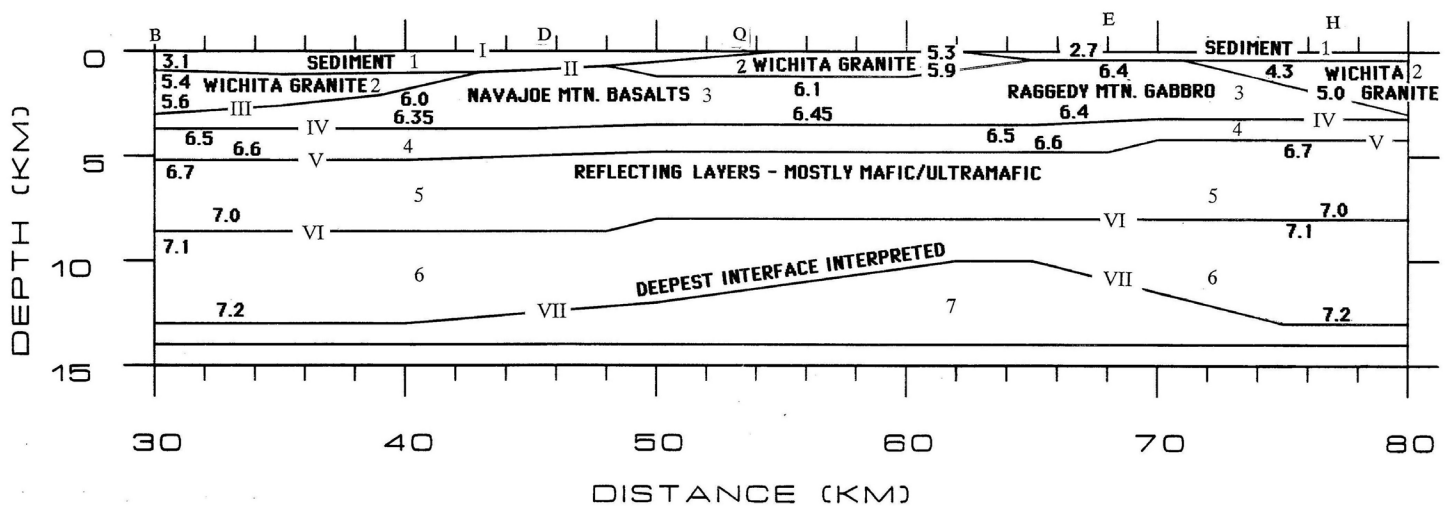


Figure 4. Hamilton's (1989) velocity model of the structure of the Wichita Uplift.

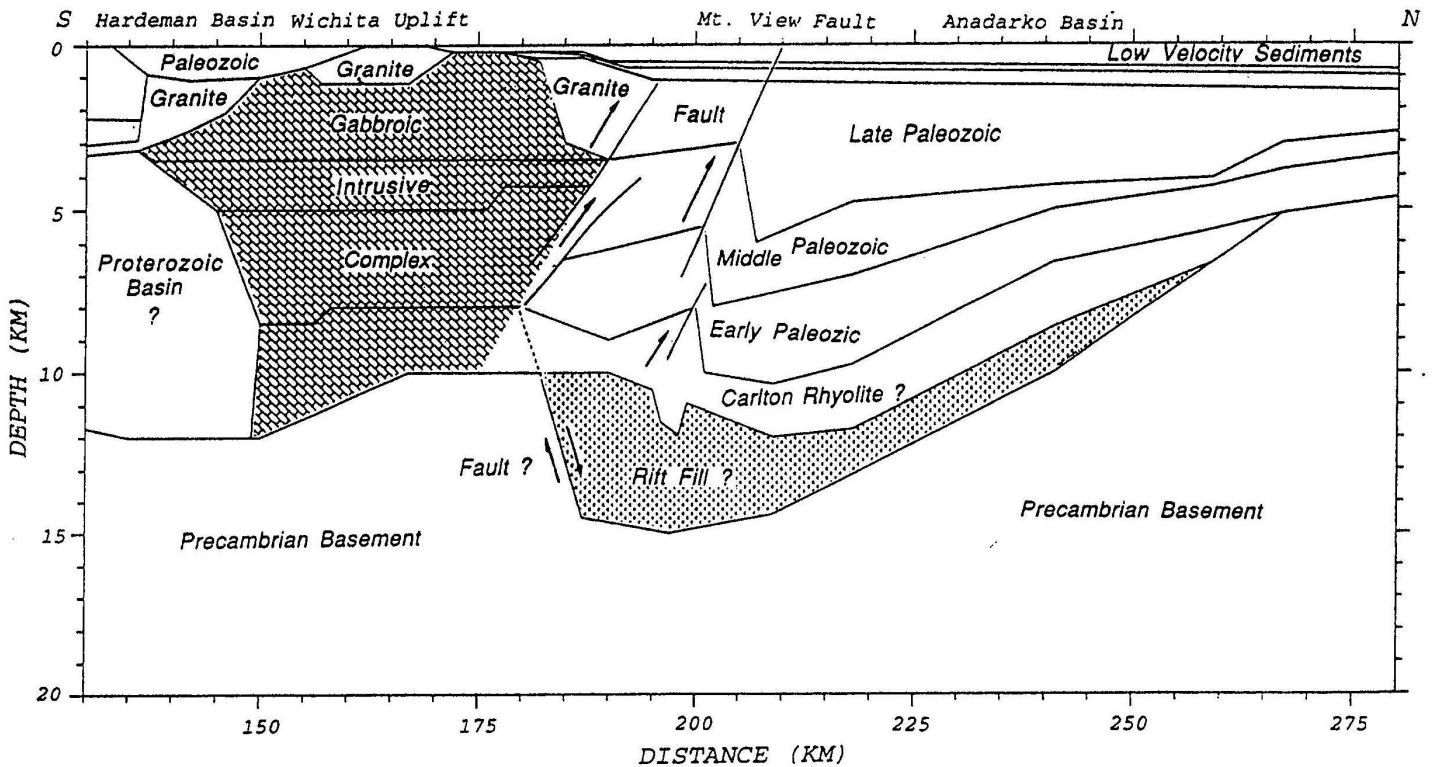


Figure 5. Hsueh's (1991) geologic interpretation of his velocity model across the Wichita Uplift and Anadarko Basin.

The upper crust-lower crust boundary varies in thickness, similar to the Moho, but the original upper crust beneath the Wichita Uplift is almost completely absent.

More recently, Keller and Stephenson (2007) revisited the classic comparison between the Southern Oklahoma and the Dniepr-Donets Aulacogens. They find that the primary differences between the rift systems are the nature of the magmatic modification of the crust and the degree of structural inversion and also provide an updated gravity model for the SOA.

Additionally, several authors have undertaken gravity and magnetic studies across the Wichita Uplift region. Lyons (1964) produced gravity maps and Jones and Lyons (1964) published magnetic maps showing linear southeast-northwest-oriented Bouguer gravity anomalies with relief in excess of 80-100 mGal and vertical magnetic maxima of up to 1400 gammas across the Wichita-Amarillo and Arbuckle Uplifts. Pruat's (1975) 2-D models propose that shallow (~2 km deep) lenticular layered bodies composed of a high-density mafic material underlie these anomalies. He also suggests that a two-km-thick basaltic layer underlying the Carlton Rhyolite compensates for the 12 km of sedimentary fill in the Anadarko Basin. Papesh (1983) proposes that the source of the anomalies lies much

deeper. His 2-D gravity models propose that a mafic pluton with a width of approximately 25 km and increasing in size to 55 km toward the southeast, is emplaced beneath the Wichita Uplift at a depth of at least 10-15 km.

Seismic Data Employed

The seismic data used in the current study was acquired in January 1985 as a joint project of the University of Texas at El Paso and the University of Texas at Dallas, with funding from a ten-member industrial consortium. The survey stretched for ~100 km from the northern end of the Hollis-Hardeman Basin, across the Wichita Uplift, and into the Anadarko Basin, passing through the same region as several of the 1979-1980 COCORP lines (Figure 6). It was designed as a wide-aperture experiment with recorder spacing intermediate between typical refraction and reflection geometries in order to study the deep structure of the Wichita Uplift, the Anadarko Basin, and the transition between them (Chang et al., 1989).

The experiment consisted of three deployments of 800 seismic group recorders with a 50% overlap between deployments. Nine in-line and two off-line shots were recorded in the first deployment, four off-line shots in the second

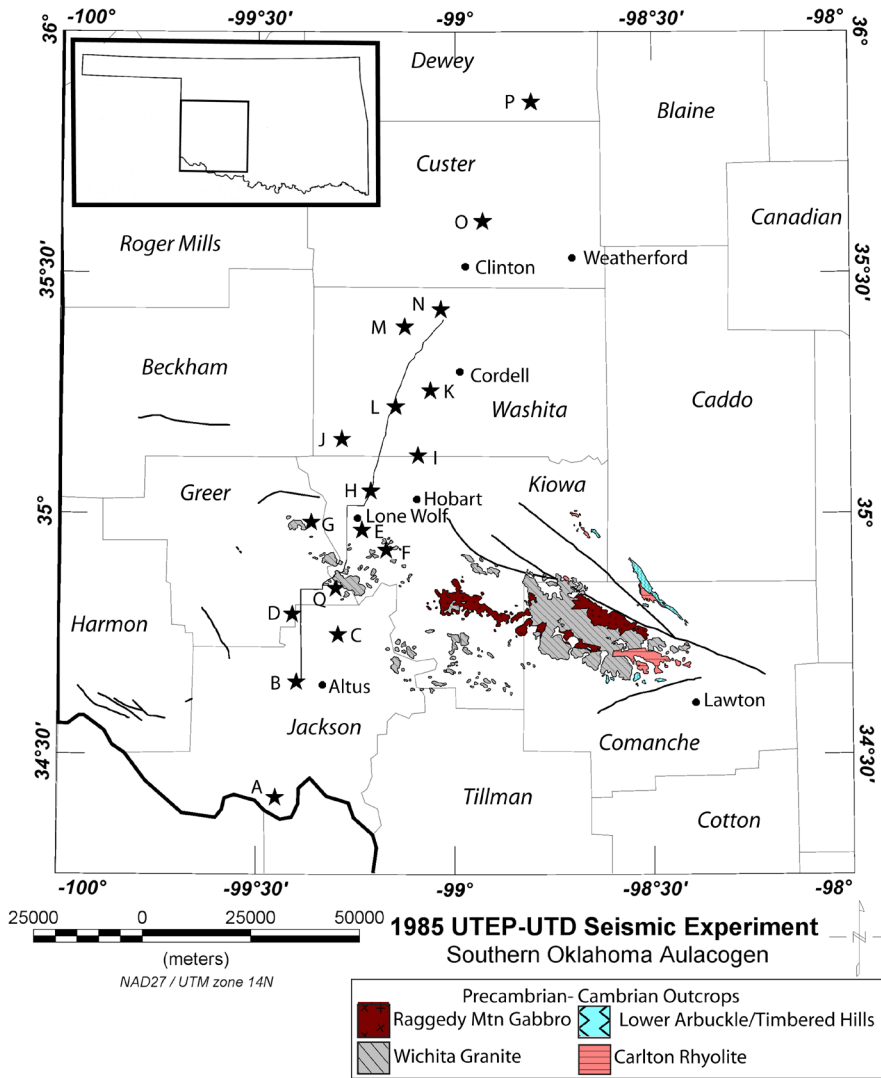


Figure 6. Shotpoint and receiver locations for the entire seismic experiment.

deployment, and eight in-line and two off-line shots in the third deployment to create three parallel lines. Six of the in-line shot locations were shot on multiple recorder deployments. Source to receiver offsets varied between 0 and 150 km, and dynamite provided the source energy. For further details on the survey, see Rondot (2009).

The primary data set used in my study consisted of the seismic shot records for shotpoints A, B, C, D, Q, E, H, and L from deployment 1 and shotpoints E, H, L, M, and N from deployment 3. I retained the original naming scheme for the shots throughout this study, with the shotpoint location designated by a letter and the number following serving as a sequential indicator of shot order. Please refer to Rondot

(2009) for images of each shot record discussed in this study.

Shot A.01 was shot across the Burch Fault at the southernmost end of the line. The nearest receivers were 27 km north of the shot on the northern side of the fault zone. Seismic control is minimal in the deeper areas of the Hardeman Basin portion of the model. I picked and modeled several reflections shallower than five sec reduced time between 27-40 km offset and identified additional reflectors to 10 sec reduced time, but did not model the latter category. Reflections shallower than five sec represent layering in the Hardeman Basin, as discussed by Brewer et al. (1981).

Shot B.06 was an in-line, nearly zero-incidence shot with an ~21-km-long straight portion before the receiver line bent. Few prominent reflectors were identifiable on the record, though I was able to pick first arrivals across nearly the entire record section. Shot C.10 was a split-spread shot located off-line to the east of the receiver line. P-wave velocities on the south side of the spread towards the Hardeman Basin were slightly slower than on the north side across the uplift. Observed and calculated first arrivals from this shot had a similar slope indicating a correct velocity match but a poor match in time. However, changing the depth to the top of layer 2 by a few tenths of a kilometer resulted in an improvement in fit for both shots A and C and a poorer match for shots B and D. I identified several prominent reflections and zones of reflectivity on this shot record, one of the most notable of which occurs between 4.0-4.5 sec at 15-20 km offset.

Shot D.09 is a split-spread shot located near the northern end of a 20-km-long straight portion of the receiver line. However, I used only picks from the north side of the spread across the uplift with a 16-km offset or greater due to an error in the file. Shot Q.03 is a split-spread shot located along a bend in the receiver line just south of a granite outcrop along the uplift. It contained several short low-amplitude reflectors but few prominent events.

Shot E.21 is positioned along the northern outcrop edge of the uplift and shot north towards the Anadarko Basin along a 50-km-long straight segment of the receiver

line. First arrivals after approximately 30 km offset were too faint to pick. Several zones of strong reflectivity are apparent on the shot record, particularly one from 1.8-2.4 sec and the other from 3.2-4.2 sec starting at 27 km offset. A steeply dipping event beginning at 3.2 sec at 14 km offset may be a reflection from the Mountain View Fault (Kang and McMechan, 1990). Shot E.05 was shot slightly offline to the south across the uplift and contained less reflectivity than shot E.21.

Shot H.22 (Figure 7) was a split-spread shot near the frontal fault zone containing strong first arrivals to the north. Several zones of reflectivity, possibly the same ones as seen on shot E.21, correspond to layering within the Anadarko Basin (Figure 8), whereas shot H.07 displays less reflectivity towards the south across the uplift. Shot L.11 is offset 25 km from the nearest receivers. The calculated first arrivals for this shot were difficult to match with the observed time picks due to a combination of the complicated fault structures traversed by the waves and the crooked-line geometry of the receivers.

Shot L.24 is a zero-offset, split-spread shot located

along a straight portion of the line. By applying a 1000 ms AGC window and a 10-55 Hz band-pass filter, the reflections seen at an offset of 3 km to the south at a time of 3.0-5.0 sec can clearly be traced back through the noise from the air blast to zero offset. Shot M.20 is one of the off-line shots employed in this study. The observed and calculated travel times for the refractions off the upper two layers in the model fit well, indicating little three-dimensional variation in this portion of the study area. Shot N.26 is located at the northern end of the receiver line. A reflector occurring at 3.2 sec at an offset of 6 km is modeled as the base of the late Paleozoic section.

Methodology

The seismic data had been well conditioned before I received it, so I performed minimal additional processing. Several programs were used in this study to work with the shot records and build the final velocity model. Much of my time working with the shot records was spent using ZPlot, a FORTRAN-based software suite for interactively plot-

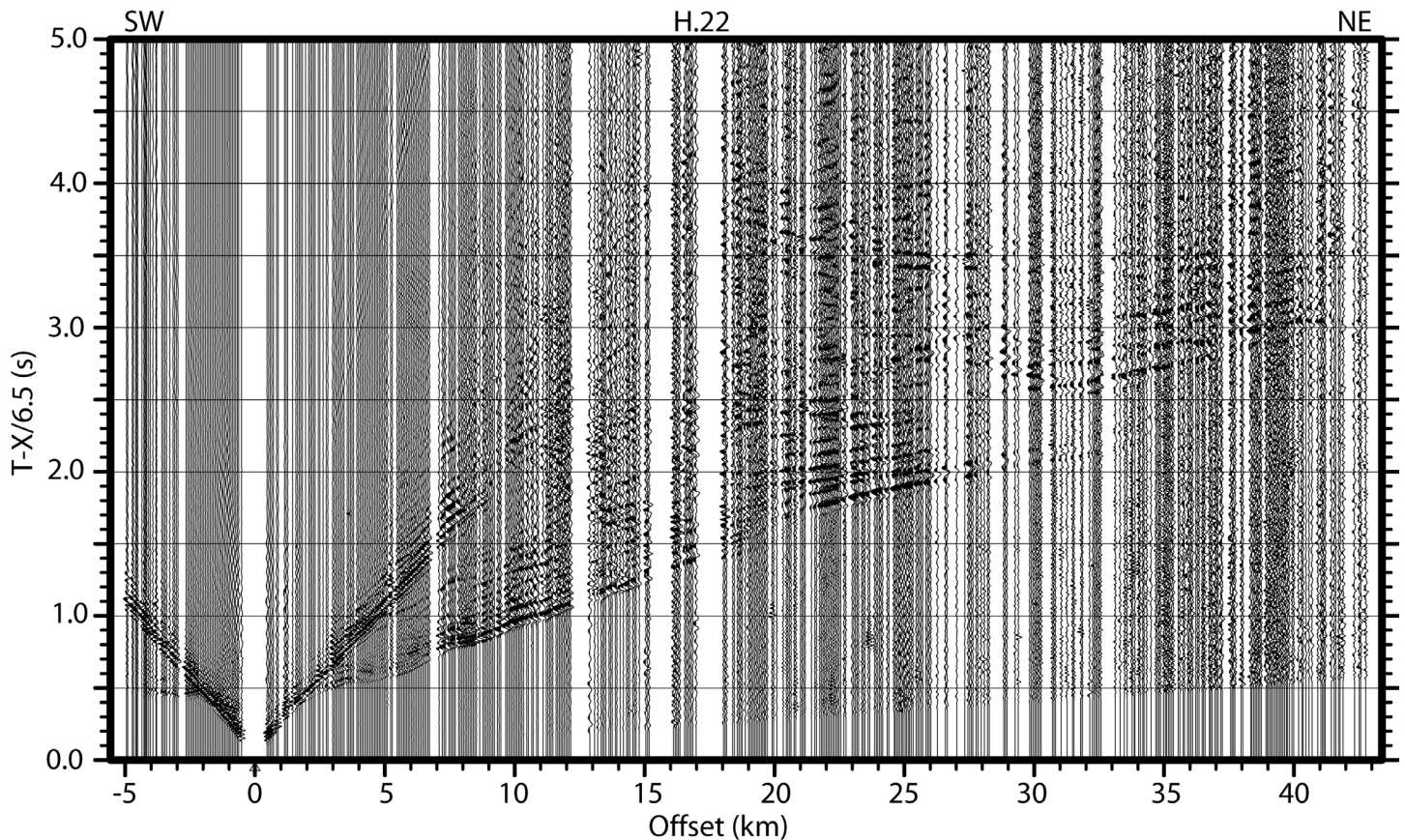


Figure 7. Shot record H.22, representative of the quality of data used in this study. Note that zero time is displayed at the bottom of the figure and times increase toward the top. All times referred to in this study are reduced times, T-X/6.5 km/sec.

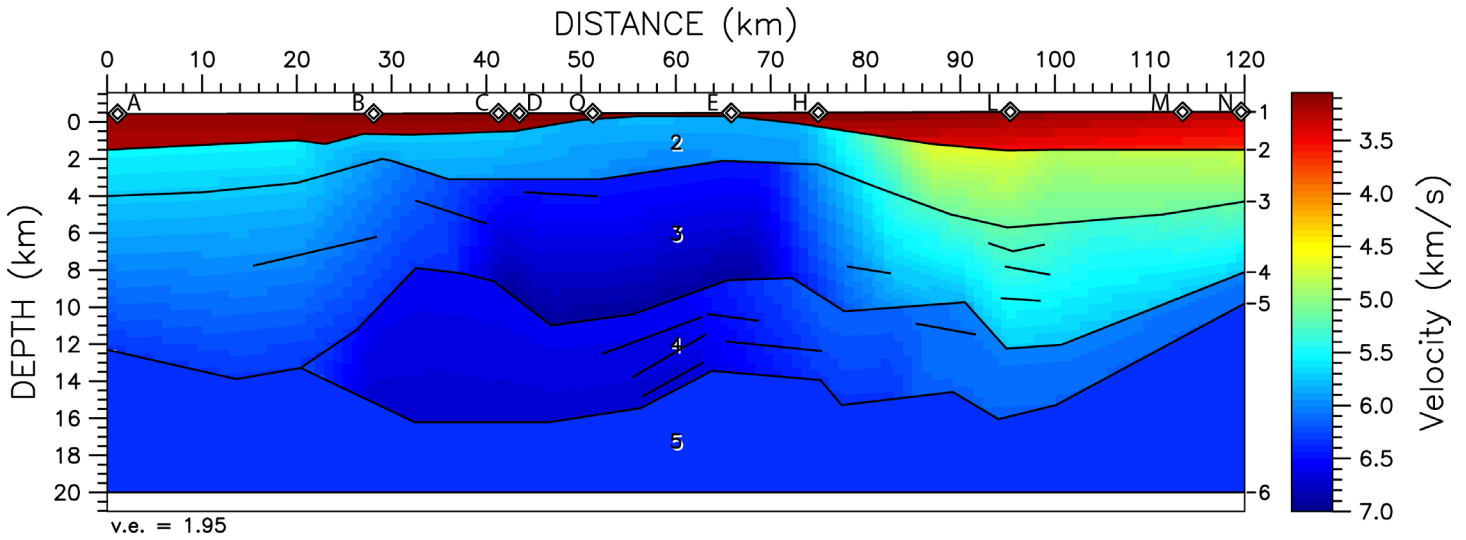


Figure 8. Close-up of reflectivity on shot H.22.

ting and picking SEG-Y-formatted seismic data (<http://www.soest.hawaii.edu/users/bzelt/zp/zp.html>). After importing the SEG-Y files and converting them to the internal ZPlot format, I plotted the data using a reduction velocity of 6.5 km/s. I picked first arrivals on all the shot records used, though I did not pick the entirety of some records due to signal-to-noise problems. ZPlot is capable of plotting the seismic traces by offset, so events retained their proportional spacing instead of being plotted equidistant by trace number. In order to accentuate the first arrival, I applied top and bottom mutes to the surrounding data, applied AGC with a window length between 500 and 1000 ms to the data, and band-pass filtered the data, generally between 4-40Hz.

Additionally, I was able to identify and pick reflections on several of the shot records. I aimed to pick the longest, most continuous reflections I could follow or the top and base of a highly reflective zone. Though reflections continued much deeper in the seismic record, I limited this study to modeling reflections which plotted five sec (approximately 20 km) deep or shallower in reduced time.

I performed trial-and-error velocity modeling of the data set using the programs VMED (<http://www.soest.hawaii.edu/users/bzelt/vmed/vmed.html>) and RAYINVR (<http://zephyr.rice.edu/departament/faculty/zelt/rayinvr.html>) (Zelt and Smith, 1992). VMED is used to build and edit the velocity model, whereas RAYINVR performs ray tracing. Picks are easily exported from the ZPlot seismic display and picking program and converted to a format readable by VMED and RAYINVR.

I built my velocity model in VMED by constructing a text file specifying the x-coordinate, depth, velocity at the top of the layer and velocity at the bottom of the layer at

nodes across a layer. Velocities can vary both vertically and laterally throughout the model or be held constant within a layer. The program allows for velocity discontinuities at layer boundaries but does not require them. Layers are also allowed to laterally pinchout by reducing the thickness to zero (Zelt and Smith, 1992). Rondot (2009) contains further details on how to construct the model.

RAYINVR traces rays in a 2-D isotropic medium using the model built in VMED and the picks chosen in ZPlot. RAYINVR is capable of tracing refracted, reflected, and head waves, including conversions. It performs both forward modeling and inversion of refraction and reflection traveltimes. RAYINVR separates the model into irregular trapezoidal blocks with vertical left and right sides and sloping tops and bottoms. By extrapolating the velocities at each corner of the block, a linearly varying velocity field is created within each block and velocity discontinuities are smoothed. The ray angles may be specified by the user and can be shot at any angle (Zelt and Smith, 1992).

Velocity Model

My initial velocity model utilized geologic constraints from the literature and was based on simplified versions of the models of Hamilton (1989), Hsueh (1991), and Suleiman (1993). The thickness of the sedimentary fill overlying the uplift was constrained by drilling results (Campbell and Weber, 2006). Depths to the major age divisions in the Anadarko Basin agree well with the depths encountered in the Lone Star No. 1 Bertha Rodgers well (sec. 27, T. 10 N., R. 19 W.), located near 102 km along the model. The positions of the main faults bounding the uplift were con-

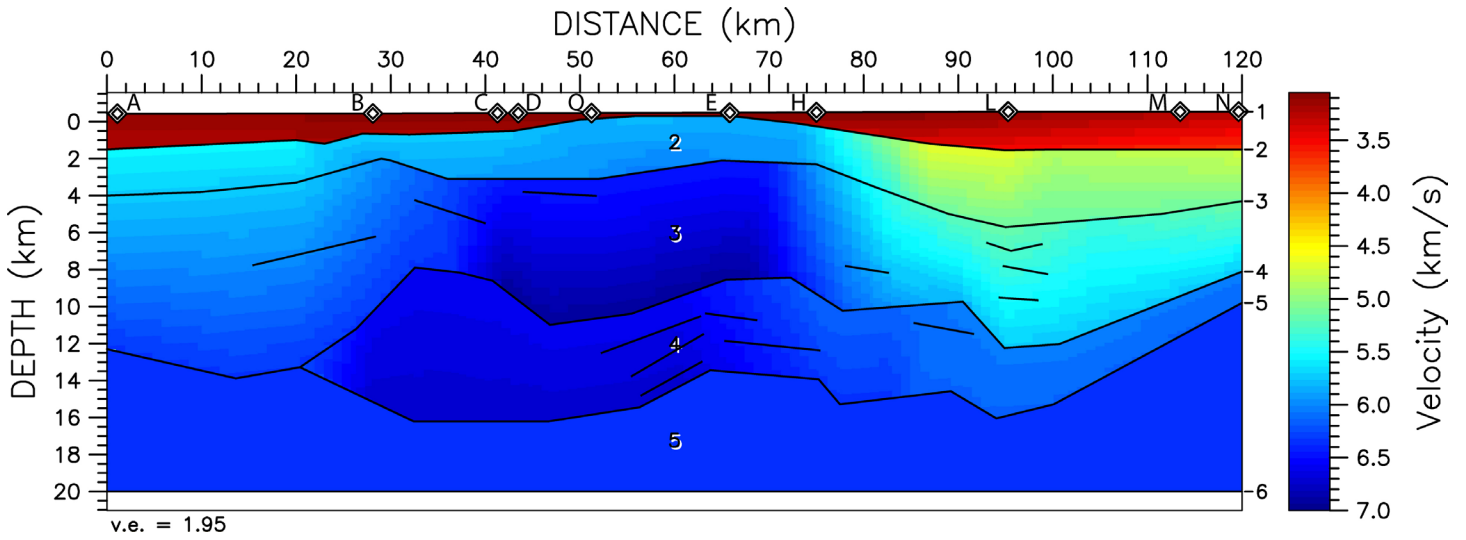


Figure 9. Final seismic velocity model with “floating” reflection boundaries.

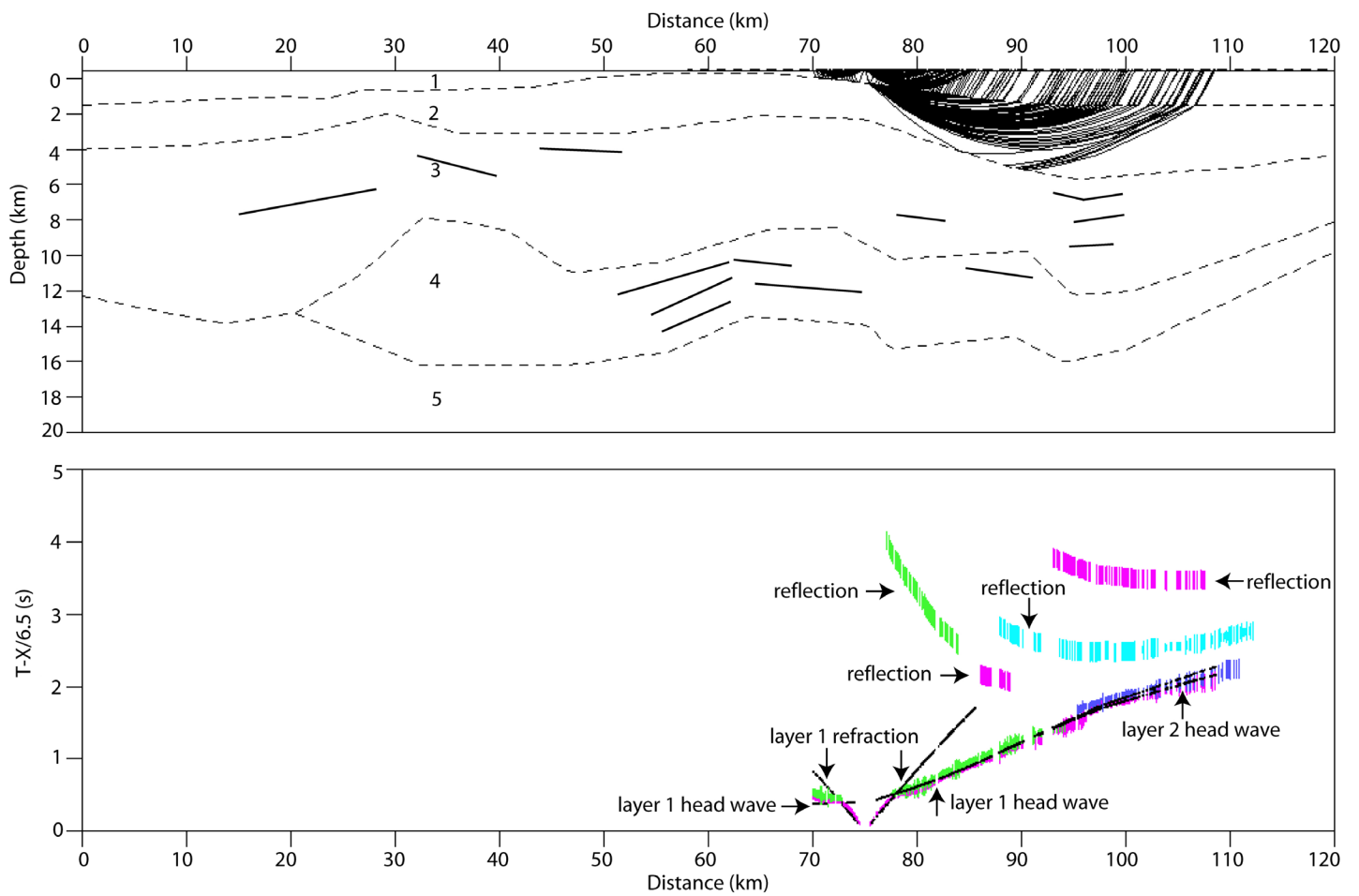


Figure 10. Refraction and head-wave coverage for layers 1 and 2 on shot H.22. Observed time picks are shown in color with the height scaled by the uncertainty calculated by ZP. Calculated times are shown as a thin black line. Every fourth ray is shown for clarity.

strained using lines 1 and 2-2A of the 1970-1980 COCORP results (Brewer et al., 1981, 1983).

Through iterative trial-and-error modeling of observed times with calculated times, I refined and augmented the initial model to arrive at my final velocity model (Figure 9). The slope of the calculated times in relation to the slope of the observed picks indicated whether the trial velocity used was too fast, too slow, or accurate, whereas the position of the observed time indicated whether the trial boundary was too deep, too shallow, or accurate. I first attempted to fit the velocities with minimal adjustment of the boundary depths then refined the depths to match the calculated and observed times, though the two processes were not mutually exclusive.

Ray coverage varied along the model, though layers 1 and 2 were well covered overall. A ray-trace diagram for shot H.22 illustrates the typical level of refraction and head-wave coverage across layers 1 and 2 of the model (Figure

10). The depths and velocities along layers 1 and 2 of the model were constrained using refracted and head waves.

The depths for layers 3, 4 and 5 were found by matching reflections, particularly those that were identifiable on multiple record sections (Figure 11). Velocities in layers 3, 4 and 5 are consequently less well constrained than in the upper two layers. Reflections that were only identifiable on one or two shot records or were part of a series bounded by more prominent reflections are modeled using short (<15 km) “floating” boundaries. No velocity discontinuity in the model is associated with this type of boundary (Zelt and Forsyth, 1999).

The velocities determined in my final model indicate probable lithologies (Christensen, 1982). Layer 1, encompassing the surface of the model down to 1.5 km deep, is a loosely consolidated sedimentary layer based on its velocity range of 3.05 to 3.75 km/s. Layer 2 from 0 km to 28 km along the model corresponds to the Hardeman Basin. The

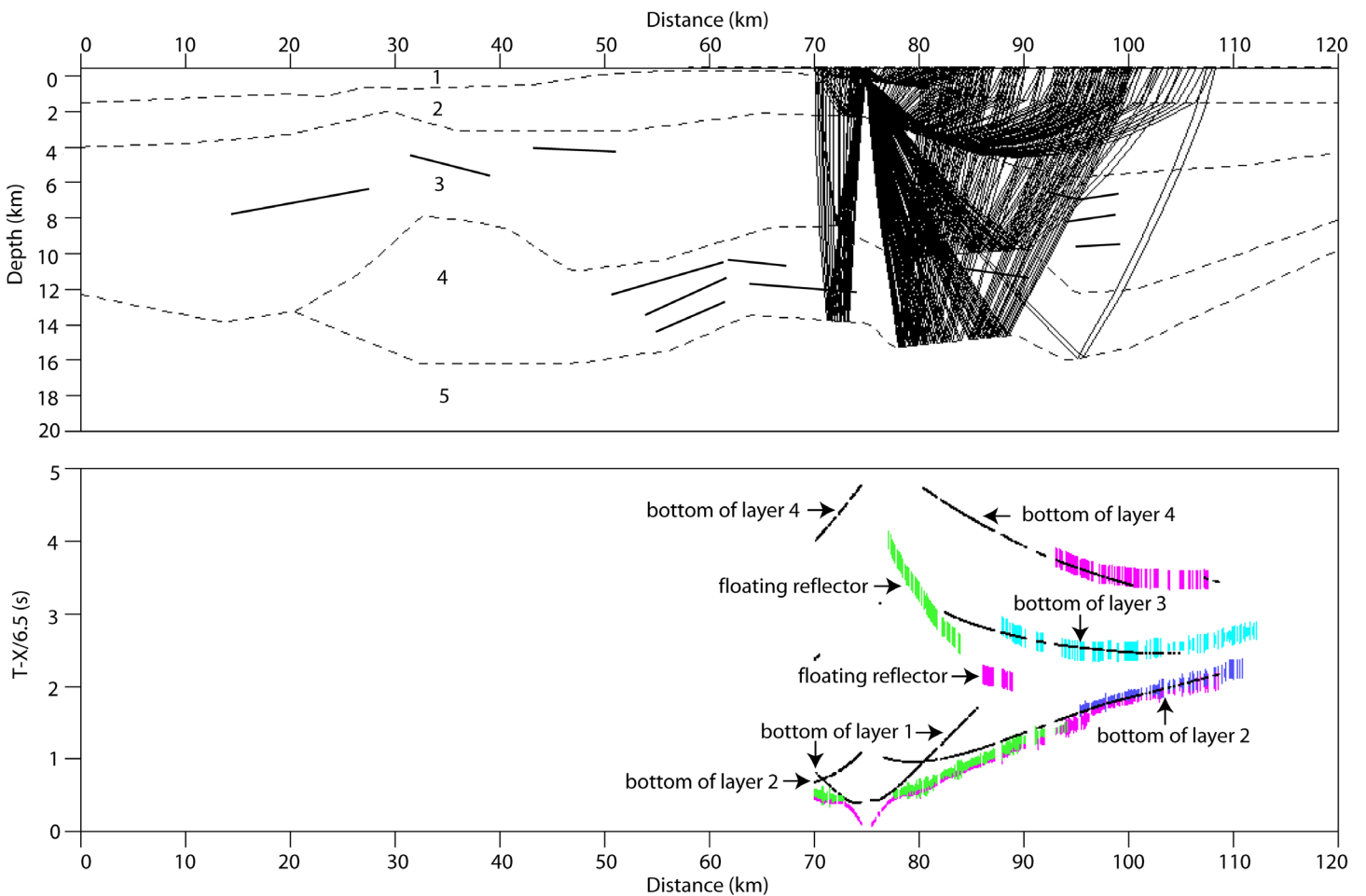


Figure 11. Raypaths of reflections from boundaries for layers 1-4 on shot H.22. Calculated times for floating boundaries are not shown. Observed time picks are shown in color with the height scaled by the uncertainty calculated by ZP. Calculated times are shown as a thin black line. Every fourth ray is shown for clarity.

velocities range from 5.60 to 5.80 km/s, representing consolidated sediments. Layer 3 from 0 km to 30 km along the model represents the Proterozoic basin discussed by Brewer et al. (1981). A lithologic determination for this layer is ambiguous based on velocity data alone, as the velocities in the basin range from 5.80 to 6.40 km/s and could represent metasediments, granites, or interlayered graywackes and basalts (Brewer et al., 1981).

The Wichita Uplift extends from approximately 30 km to 80 km along the model. Layer 2 exhibits velocities ranging from 5.80 to 6.10 km/s. In conjunction with outcrop data, this layer can be identified as primarily granite and rhyolite. The high velocities of layer 3, ranging from 6.50 to 7.00 km/s, are indicative of mafic igneous rocks such as gabbro and basalt. Velocities in Layer 4 in the distance range of 20 km to 47 km may be representative of Precambrian upper crust, though these values are poorly constrained. The region from 47 km to around 80 km along the model likely is a mafic layered complex based on the velocities ranging from 6.65 to 6.80 km/s and the numerous reflections modeled.

The Anadarko Basin extends from 80 to 120 km on my model, with the frontal fault zone from 78 km to 98 km serving as a transition zone between the uplift and the Anadarko Basin. Velocities of layer 2 range from 4.70 to 5.20 km/s. Based on drilling data, this layer can be identified as primarily sandstones and shales. Layer 3 displays velocities from 5.20 to 5.80 km/s and can be identified from drilling results as primarily limestone. Layer 4 has velocities of 6.10 to 6.20 km/s, though these are not well constrained, which may represent either limestone or rift fill from the earliest history of the basin. Finally, layer 5, which extends across the entire model, has a velocity of 6.40 km/s and is interpreted as Precambrian upper crust.

I was unable to identify reflections in Layer 2 of the Wichita Uplift, confirming the observations of previous studies that this area is nearly seismically transparent (McMechan et al., 1985; Brewer et al., 1983). In addition to the reflections modeled, layer 3 contained several reflections that I did not pick. These reflections may be interfaces between distinct pulses of mafic material. Numerous reflections are present in layer 4, consistent with it containing a layered mafic complex. Reflections

beyond 76 km along the model correspond to sedimentary layering within the Anadarko Basin. Reflections from 0 to 30 km are layering in the Proterozoic basin discussed by Brewer et al. (1981), but provide no new information to confirm lithologies.

Petroleum Geo-Services (PGS) Onshore, now owned by Geokinetics, generously provided screenshots of two vertical time slices approximately along my shotpoint lines from their Wichita Mountain Front 3D seismic-reflection surveys. The time-migrated data image complicated thrust structures across the frontal fault zone that are well below the resolution of my model, serving to constrain fault locations in my model. A positive flower structure can be identified on one of the lines, offering evidence of oblique slip along the frontal fault zone.

Gravity And Magnetic Data And Modeling

I used the Oasis Montaj software to map gravity and magnetic variations within the study area and GM-SYS

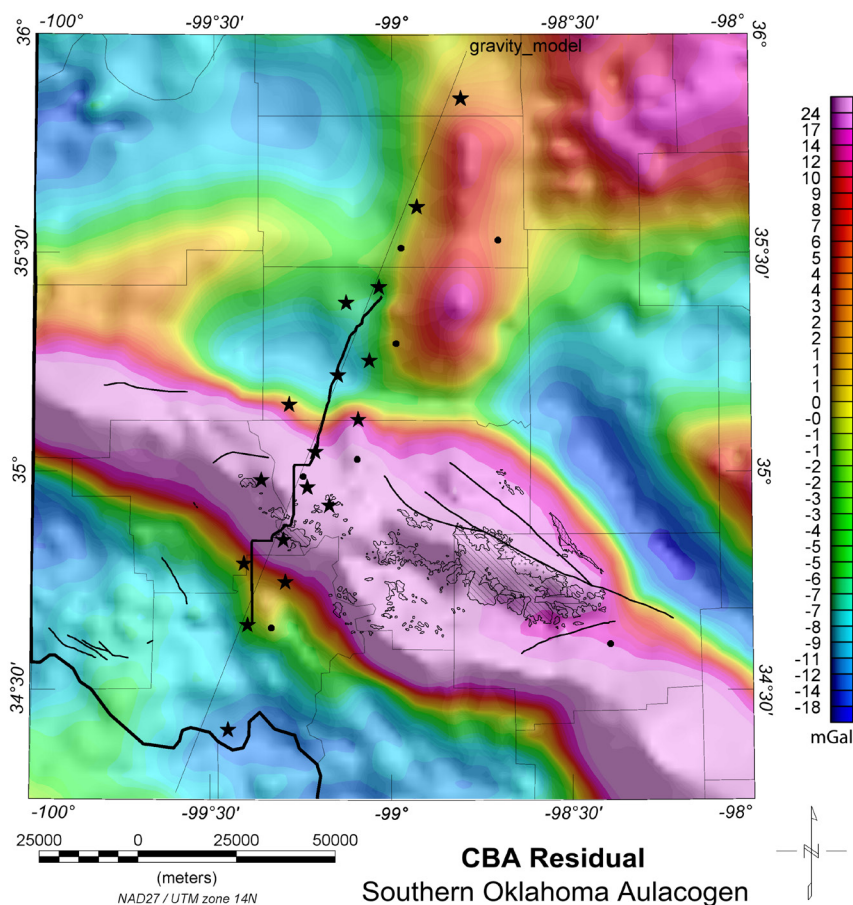


Figure 12. Residual Bouguer gravity anomaly showing areas of dense igneous rocks corresponding to the SOA.

to model the gravity variations along a profile roughly coincident with the seismic line. The data came from several sources. Gravity readings were downloaded from the PACES website (research.utep.edu/paces). Magnetic readings for Oklahoma were downloaded from the USGS state compilations website. Digital elevation measurements also were downloaded from the USGS. All data were reprojected to the NAD27 datum, UTM zone 14N.

Gridding and contouring the complete Bouguer anomaly (CBA) reveals a variation of approximately 170 mGals across the southwestern Oklahoma and northwestern Texas region, with the SOA delineated as a northwest-trending gravity high. Next, I upward continued the data to 20 km above the Earth's surface. Upward continuation acts as a type of low-pass filter to attenuate shorter-wavelength anomalies and smooth the data (Blakeley, 1996). The residual Bouguer anomaly grid was calculated by point-by-point subtraction of the upward continued grid from the CBA grid, thus removing the long-wavelength deep anomalies from the data and accentuating shallower features. As shown in Figure 12, the range of the gravity anomalies is narrowed to 42 mGals, though the Wichita Uplift still appears as a strong northwest-trending high. Strong gravity lows corresponding to the Anadarko and Ardmore Basins are visible on the northern side of the Wichita Uplift, and a low corresponding to the shallower Hardeman Basin occurs to the south of the uplift.

In an attempt to delineate the faults surrounding the Wichita Uplift, I calculated the horizontal gradient magnitude (HGM) on the Bouguer gravity residual (Figure 13). The HGM takes the first derivative of the gravity or magnetic measurement with respect to both the x and y directions. It is sensitive to lateral discontinuities, making it a useful edge detector. The steepest gradients tend to correspond to the edges of a body (Blakeley, 1996). The HGM map shows that the Wichita Uplift is not a single homogeneous anomaly as suggested by the CBA residual map, but is rather made up of discrete igneous bodies and separated by complex fault zones. In particular, the location of the Mountain View Fault can be interpreted from the map. I also calculated the tilt derivative, a ratio of the first vertical and total horizontal deriv-

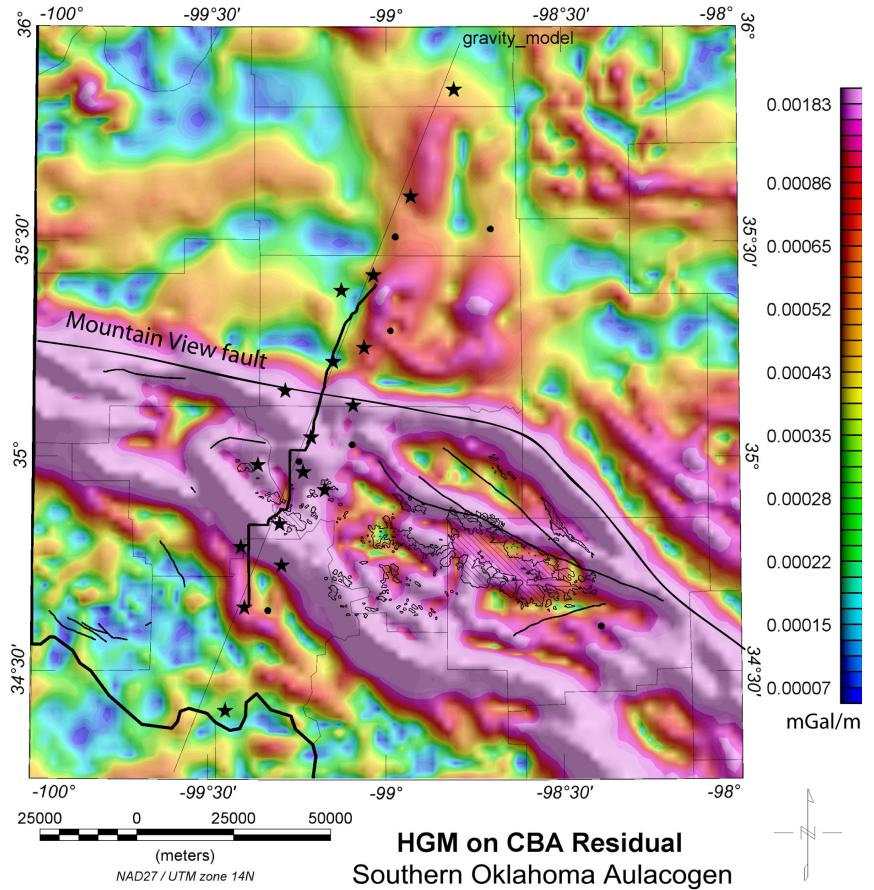


Figure 13. Horizontal gradient magnitude calculated on the Bouguer gravity residual. Edges corresponding to discrete igneous bodies are enhanced as maxima. Interpreted location of the Mountain View Fault is shown by the thick black line.

atives, on the Bouguer gravity residual to further delineate structures.

Next, I gridded the total magnetic intensity (TMI) and reduced it to the pole (Figure 14). Unlike the gravity field, the direction of the magnetic vector differs with latitude and does not always point vertically. Reduction-to-pole centers the magnetic anomaly over its causative source (Blakeley, 1996) as long as any remnant magnetism is weak. The TMI-reduced-to-pole map displays a less homogeneous anomaly corresponding to the SOA than does the CBA gravity residual map, likely corresponding to the locations of mafic blocks adjacent to felsic or sedimentary bodies.

The main value of the maps was to help locate lithologic and fault boundaries in my gravity model. The maps based on magnetic data provided information on the locations and edges of mafic bodies in particular, which tend to have a higher magnetic susceptibility than felsic or sed-

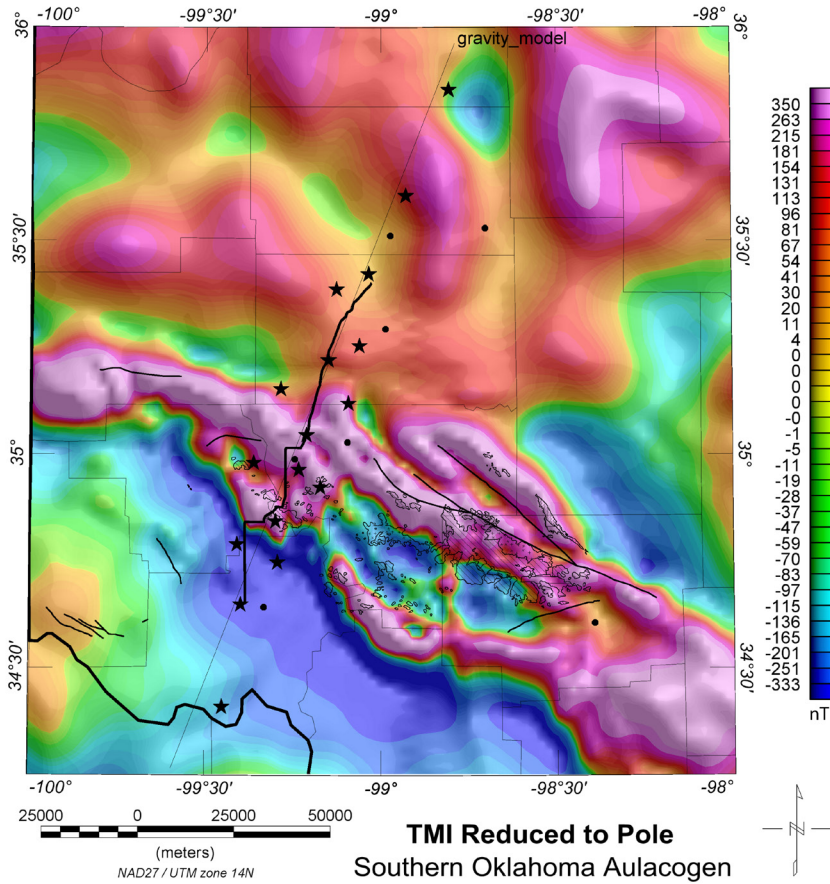


Figure 14. Total magnetic intensity reduced to the pole. Areas of high magnetic susceptibility, corresponding to primarily mafic rocks, are outlined along a northwest trend.

imentary rocks. The gravity maps help define the boundaries of igneous rocks associated with the SOA. The horizontal-gradient-maximum and the tilt-derivative maps were particularly useful for defining fault locations.

I constructed a preliminary gravity model approximately halfway through the seismic modeling process and used this to guide my seismic modeling, and then the final gravity model was built using the depth boundaries I found in my final seismic model. I held these depths constant in the gravity model, so the only variables were density and the locations of boundaries between blocks. Densities were first assigned using an empirical formula relating density with velocities found in my seismic model (Brocher, 2005). Lateral boundaries between blocks corresponding to faults or lithologic changes were added based on boundaries observed on the gravity and magnetic maps. I then adjusted the locations of these boundaries within approximately ± 2 km, adjusted densities within approximately ± 0.1 g/cm³, and

added more blocks as needed until the observed and calculated gravity fit within 10 mGals. I did not attempt to model the observed magnetic data as magnetic susceptibilities for a given rock type often vary over several orders of magnitude, but rather used these data to understand where small shallow mafic bodies may be located.

My final gravity model shows my lithologic interpretations based on densities (Christensen, 1982) and the known geological history of the SOA (Figure 15). The “metasediments” and “rift fill” designations are tentative identifications of these units. The deep (10 km) metasedimentary block 40-65 km along the model may instead be Precambrian upper crust deformed during rifting and subsequent inversion of the SOA, as the bottom and southwest boundaries used were not constrained in the seismic modeling. Additionally, the lithologies of the blocks in the frontal fault zone from approximately 85 km to 110 km along the model are ambiguous. Based on the seismic data provided by PGS, they are probably granite and rhyolite mixed with the adjacent sedimentary rocks, juxtaposed by the many faults in the area.

Although the granite and rhyolite are identified as separate blocks based on geological constraints, a similar fit would have been achieved by treating them as one unit. Conversely, the magnetic data indicate that the shallow (~ 1 km deep) mafic body located at 75 km along the model is actually a series of separate bodies instead of the continuous body I modeled to fit to the gravity data. The two deeper mafic complexes account for much of the gravity high across the profile.

Interpretations And Conclusions

Using modern software packages and processing techniques, I was able to identify more phases and reflections in the 1985 UTEP-UTD seismic data set than had been previously been possible. By including several offline shots in my ray-trace model, I produced a generalized pseudo-3D model of the upper crustal structure under the Wichita Uplift and the adjoining portions of the Hardeman and Anadarko Basins.

I integrated the results from my seismic-velocity model with my gravity model, the high-quality industry seismic-reflection images from PGS, and prior geological constraints to arrive at a geological interpretation of the study

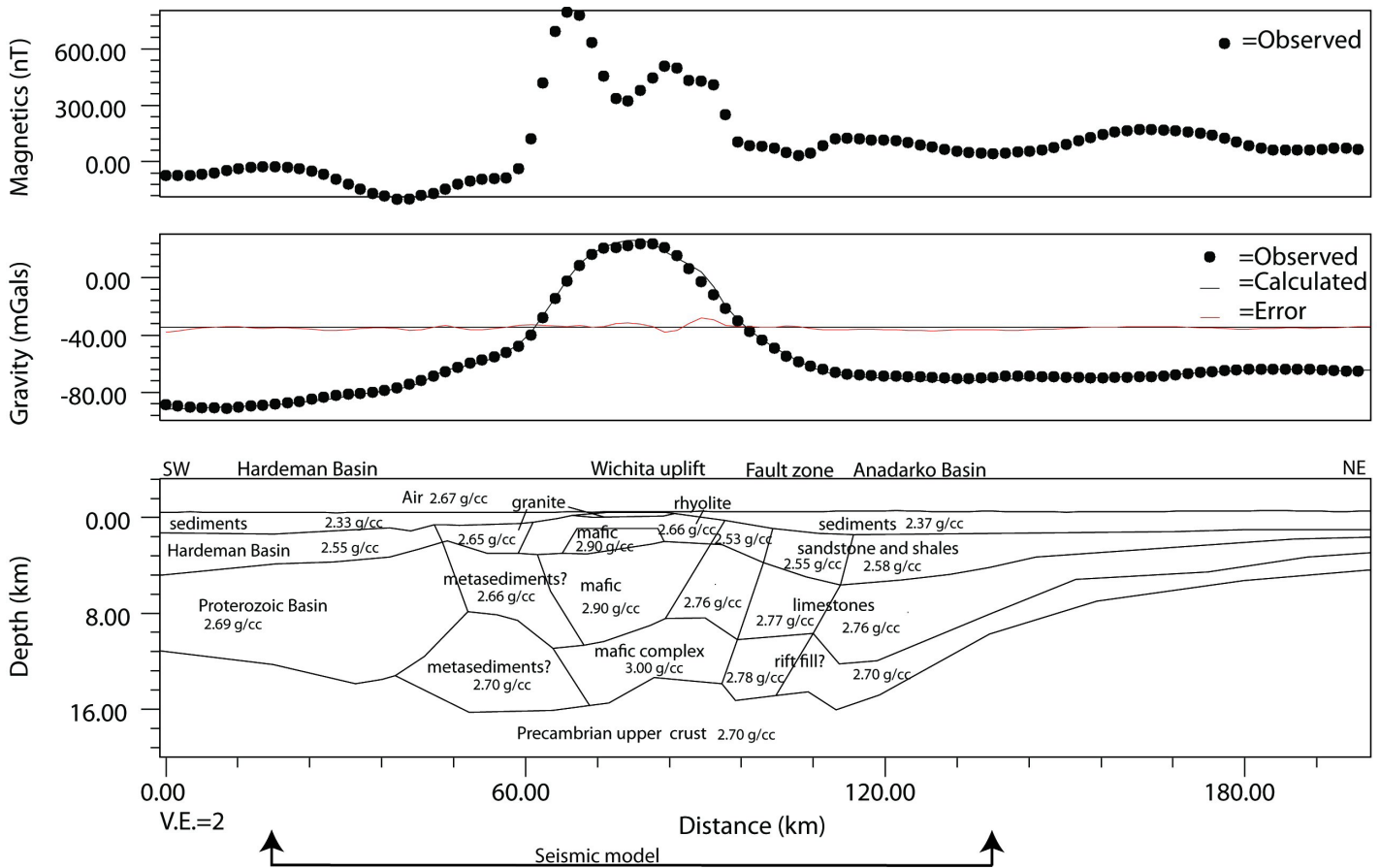


Figure 15. Gravity model across the profile indicated on the preceding maps. Densities are given in grams per cubic centimeter, and the likely composition is listed for most blocks. Observed magnetic data are shown but not modeled.

area (Figure 16). Depth boundaries were found using my seismic data set, and lithologies were determined using both the seismic velocities and densities of the rocks. The gravity mapping and modeling helped locate faults and the boundaries between lithologic units, and fault locations in the northern half of the model are further constrained from the PGS reflection lines.

The final geologic model shows that the sequence of granite and rhyolite sequence present beneath the uplift is thicker than previously modeled, 2.5 km thick in my model versus 1.5 km thick in Hsueh's (1991) model. Thick sequences of what may be the 1.2-1.4 Ga Tillman metasediments are present adjacent to the Proterozoic basin at the southern end of the model. Dense mafic layers extending to a depth of 15 km form the core of the uplift, revealing the impressive scale of crustal modification in the rifting process.

Using the industry reflection data, I was able to more accurately identify fault locations within the frontal fault zone on the northern end of the model than had been done

on previous models. High-resolution gravity and magnetic maps assisted greatly in confirming fault locations. Although I identified the fault with the most vertical separation as the Mountain View Fault, the area is a fault zone with complex branching faults. Over 12 km of relief exists between the Wichita Uplift and the Anadarko Basin, attesting to the large scale of movement along this fault system. The location of the Mountain View Fault and surrounding fault zone corresponds within with the location determined by Brewer et al. (1983) and Chang et al. (1989). Furthermore, I identified a large fault at x=100 km along the model, well into the Anadarko Basin, that clearly shows evidence of oblique motion.

Brewer et al. (1983) interpreted a fault, which they identified as the Meers Fault, at a position equivalent to x=76 km along my model. However, I found no evidence in the gravity or magnetic maps to indicate that the Meers Fault continues into the study area from its mapped location to the east.

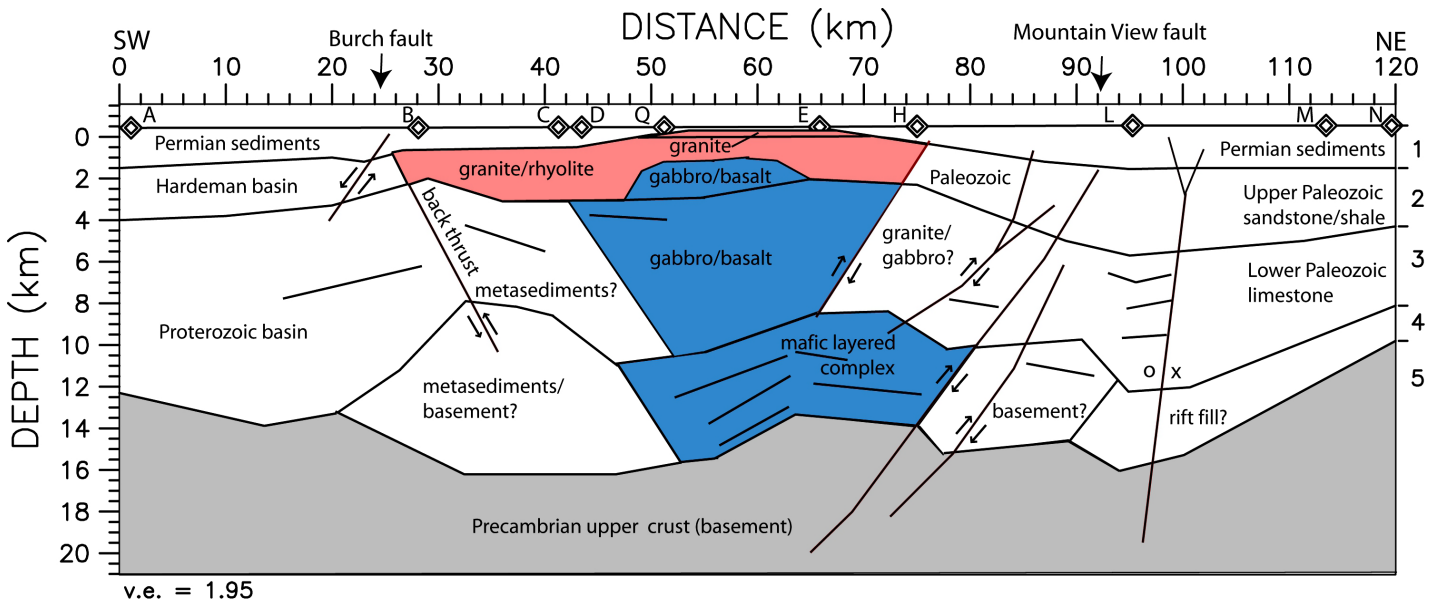


Figure 16. Integrated geological interpretations across the Southern Oklahoma Aulacogen. Faults are shown in red, boundaries between lithologic units are shown as black near-vertical lines, and reflectors are shown as black sub-horizontal lines.

The synthesis of fault interpretations by Campbell (2007) assisted in identifying fault locations to the south of the uplift. Drilling data indicates that the Burch Fault is a small-scale down-to-the-south normal fault, not a reverse fault like the faults north of the uplift. Consistent with Campbell's (2007) interpretation, my results show that the main boundary between the Wichita Uplift and the basins to the south is the fault identified as a back thrust rather than the Burch Fault as indicated by Brewer et al. (1981).

By overlaying the PGS reflection lines on the boundaries and reflectors from my velocity mode, I was able to confirm the accuracy of my model in the Anadarko Basin for a series of reflectors 6.5 to 10 km deep. The orientation and approximate locations of three short reflectors located below shotpoint L match well with the reflectivity series shown on the reflection data, increasing my confidence in the fit of the model in other locations.

The primary new results of my analysis are: 1) I employed more shots records than previously used in a single study of this dataset, 2) I used modern software and techniques to identify more phases in the data, including reflections, than done in previous studies, 3) I identified more fault locations with greater accuracy, and 4) I integrated more data types to constrain the model. As a result, I produced a considerably more detailed geologic model of the upper crust than had previously been done using this data set.

REFERENCES CITED

Blakley, R.J., 1996, *Potential Theory in Gravity and Magnetic Applications*: Cambridge, UK, Cambridge University Press, 441p.
 Brewer, J.A., Brown, L.D., Steiner, D., Oliver, J.E., and Kaufman, S., 1981, Proterozoic basin in the southern Midcontinent of the United States revealed by COCORP deep seismic profiling: *Geology*, v. 9, p. 569-575.
 Brewer, J. A., Good, R., Oliver, J.E., Brown, L.D., and Kaufman, S., 1983, COCORP profiling across the Southern Oklahoma Aulacogen; overthrusting of the Wichita Mountains and compression within the Anadarko Basin: *Geology*, v. 11, p. 109-114.
 Brocher, T.M., 2005, Empirical relations between elastic wavespeeds and density in the Earth's crust: *Bulletin of the Seismological Society of America*, v. 95, p. 2081-2092.
 Budnik, R.T., 1986, Left-lateral intraplate deformation along the Ancestral Rocky Mountains: Implications for late Paleozoic plate motions: *Tectonophysics*, v. 132, p. 195-214.
 Burke, K., 1977, Aulacogens and continental breakup: *Annual Review of Earth and Planetary Science*, v. 5, p. 371-396.
 Burke, K., and Dewey, J.F., 1973, Plume-generated triple junctions: Key indicators in applying plate tectonics to old rocks: *Journal of Geology*, v. 81, p. 406-433.
 Campbell, J.A., and Weber, J.L., 2006, *Wells Drilled to Basement in Oklahoma*: Oklahoma Geological Survey Special Publication 2006-1, unpag.
 Campbell, J.A., 2007, Understanding the structure of the Wichita Uplift, southern Oklahoma: *Shale Shaker*, v. 58, p. 87-97.
 Chang, W.F., McMechan, G.A., and Keller, G.R., 1989, Wavefield processing of data from a large-aperture seismic experiment in southwestern Oklahoma: *Journal of Geophysical Research*, v. 94, p. 1803-1816.
 Christensen, N.I., 1982, Seismic velocities, in Carmichael, R.S., ed., *Handbook of Physical Properties of Rocks Volume II*: CRC Press,

Geophysical analysis of crustal structure in Wichita region

- Boca Raton, FL, p. 1–228.
- Feinstein, S., 1981, Subsidence and thermal history of Southern Oklahoma Aulacogen: implications for petroleum exploration: *American Association of Petroleum Geologists Bulletin*, v. 65, p. 2521-2533.
- Gilbert, M.C., 1983, Timing and chemistry of igneous events associated with the Southern Oklahoma Aulacogen: *Tectonophysics*, v. 94, p. 439-455.
- Gilbert, M.C., and Hogan, J.P., 1995, Wichita Mountains Field Trip: May 26-28, 1995: 12th International Conference on Basement Tectonics, 50p.
- Ham, W.E., Denison, R.E., and Merritt, C.A., 1964, Basement Rocks and Structural Evolution of Southern Oklahoma: *Oklahoma Geological Survey Bulletin* 95, 302p.
- Hamilton, L.S., 1989, Structure of the Wichita Uplift, southern Oklahoma, from a wide-angle seismic experiment [M.S. thesis]: El Paso, Texas, University of Texas at El Paso, 89p.
- Hoffman, P., Dewey, J.F., and Burke, K., 1974, Aulacogens and their genetic relations to geosynclines, with a Proterozoic example from Great Slave Lake, Canada, *in* Dott, R. J., Jr., and Shaver, R. H., eds., *Modern and Ancient Geosynclinal Sedimentation*: Society of Economic Paleontologists and Mineralogists Special Publication 19, p. 38-55.
- Jones, V.L., and Lyons, P.L., 1964, Vertical Intensity Magnetic Map of Oklahoma: Oklahoma Geological Survey Map GM-6, scale 1:750,000.
- Hsueh, Fu-Jen, 1991, Application of ray trace modeling to a large scale seismic experiment in Oklahoma [M.S. thesis]: El Paso, Texas, University of Texas at El Paso, 94p.
- Kang, I.B., and McMechan, G.A., 1990, Two-dimensional elastic pseudo-spectral modeling of wide-aperture seismic array data with application to the Wichita Uplift-Anadarko Basin region of southwestern Oklahoma: *Bulletin of the Seismological Society of America*, v. 80, p. 1677-1695.
- Keller, G.R., Lidiak, E.G., Hinze, W. J., and Braile, L.W., 1983, The role of rifting in the tectonic development of the Midcontinent, U.S.A.: *Tectonophysics*, v. 94, p. 391-412.
- Keller, G.R., and Stephenson, R.A., 2007, The Southern Oklahoma and Dniepr-Donets Aulacogens: a comparative analysis, *in* Hatcher, R.D., ed., *4-D Framework of Continental Crust*: Geological Society of America Memoir 200, pp. 127-143.
- Kluth, C.F., and Coney, P.J., 1981, Plate tectonics of the Ancestral Rocky Mountains: *Geology*, v. 9, p. 10-15.
- Larson, E.E., Patterson, P.E., Curtis, G., Drake, R., Mutschler, F.E., 1985, Petrologic, paleomagnetic, and structural evidence of a Paleozoic rift system in Oklahoma, New Mexico, Colorado, and Utah: *Geological Society of America Bulletin*, v. 96, p. 1364-1372.
- Lynn, H.B., 1979, Migration and interpretation of deep crustal seismic reflection data [Ph.D. thesis]: Palo Alto, California, Stanford University, 159p.
- Lyons, P.L., 1964, Bouguer Gravity Map of Oklahoma: Oklahoma Geological Survey Map GM-7, scale 1:750,000.
- McConnell, D.A., 1989, Determination of offset across the northern margin of the Wichita Uplift, southwest Oklahoma: *Geological Society of America Bulletin*, v. 101, p. 1317-1332.
- McConnell, D.A., and Gilbert, M.C., 1990, Cambrian extensional tectonics and magmatism within the Southern Oklahoma Aulacogen: *Tectonophysics*, v. 174, p. 147-157.
- McMechan, G. A., Nation, J. B., and Ward, R. W., 1985, Two-dimensional synthetic seismogram modeling of wide-angle seismic data from the Wichita Uplift, Oklahoma: *Bulletin of the Seismological Society of America*, v. 75, p. 1699-1711.
- Mitchell, B.J., and Landisman, M., 1970, Interpretation of a crustal section across Oklahoma: *Geological Society of America Bulletin*, v. 81, p. 2647-2656.
- Papesh, H., 1983, A regional geophysical study of the Southern Oklahoma Aulacogen [M.S. thesis]: El Paso, Texas, University of Texas at El Paso, 94p.
- Powell, B.N., and Phelps, D.W., 1977, Igneous cumulates of the Wichita province and their tectonic implications: *Geology*, v. 5, p. 52-56.
- Pratt, T.L., Hauser, E.C., and Nelson, K.D., 1992, Widespread buried Precambrian layered sequences in the U.S. mid-continent: evidence for large Proterozoic depositional basins: *American Association of Petroleum Geologists Bulletin*, v. 76, p. 1384-1401.
- Pruatt, M.A., 1975, The Southern Oklahoma Aulacogen: A Geophysical and geological investigation [M.S. thesis]: Norman, Oklahoma, University of Oklahoma, 59p.
- Rondot, A.N., 2009, An integrated geophysical analysis of crustal structure in the Wichita Uplift region of southern Oklahoma [M.S. thesis]: Norman, Oklahoma, University of Oklahoma, 107p.
- Shatski, N.S., 1946, The great Donets Basin and the Wichita system: Comparative tectonics of ancient platforms: *Akademiya Nauk SSR Investiga, Seriya Geologicheskaya*, v. 6, p. 57-90.
- Suleiman, A.S., 1993, Geophysics of the rifts associated with the Sirt Basin (North Africa) and the Anadarko Basin (North America) [Ph.D. thesis]: El Paso, Texas, University of Texas at El Paso, 171p.
- Tryggvason, E., and Qualls, B., 1967, Seismic refraction measurements of crustal structure in Oklahoma: *Journal of Geophysical Research*, v. 72, p. 3738-3740.
- Widess, M.B., and Taylor, G.C., 1959, Seismic reflections from layering within the Precambrian basement complex, Oklahoma: *Geophysics*, v. 24, p. 417-425.
- Zelt, C.A., and Forsyth, D.A., 1999, Modeling wide-angle seismic data for crustal structure: southeastern Grenville province: *Journal of Geophysical Research*, v. 99, p. 11687-11704.
- Zelt, C.A., and Smith, R.B., 1992, Seismic travelttime inversion of 2-D crustal velocity structure: *Geophysics Journal International*, v. 108, p. 16-34.
- Zhu, X., and McMechan, G.A., 1989, 2-D tomographic imaging of velocities in the Wichita Uplift- Anadarko Basin region of southwestern Oklahoma: *Bulletin of the Seismological Society of America*, v. 79, p. 873-887.

